Design and Implementation of a Closed-Loop Filament Extrusion System with Optical Slack Sensing

Rafael Amador
Dept. of Electrical & Computer Engineering
University of Texas at Dallas
Richardson, Texas
rfa230000@utdallas.edu

Abstract* — This report presents the completed design, fabrication, and validation of a vertically oriented, closed-loop filament extrusion system developed in the RIDE Research Laboratory at the University of Texas at Dallas. The platform reclaims and modernizes a partially functional FilaStruder–FilaWinder pair inherited from a prior researcher and replaces its open-loop, horizontally mounted predecessor with a modular ABS enclosure, a five-element LDR slack ladder illuminated by a 1 W red line laser, an AH3503 linear Hall-effect diameter sensor, and an ESP32-based control board running a single integrated firmware. The firmware implements a non-blocking state machine with debounced sensor handling, ramped step-rate control of a TMC2209-driven NEMA-17 winder, three-point quadratic diameter calibration via Lagrange interpolation, an OLED human–machine interface, and NVS persistence of all calibration and speed parameters. Closed-loop operation was validated end-to-end: an extrusion-rod restoration recovered both inherited barrels, a parameter sweep over 190–210 °C and 25–100 % winder speed identified 195 °C at maximum winder speed as the optimal operating point, and two 20-minute live runs produced approximately one meter of 1.75 mm filament per spool while streaming live diameter data to a MATLAB monitor. Within the post-calibration rolling window the diameter sensor resolves to approximately ±0.03 mm against a control spool of commercial ABS Overture filament. Remaining variance is attributable to non-uniform pull tension at the spooler rather than to the sensor or controller; a planned bearing-supported guide rail addresses this directly. The system is now in a continuous, repeatable state and is ready to support the lab's downstream work on magnetic and conductive composite filaments.

Keywords* — filament extrusion, closed-loop control, modular design, LDR sensing, automated winding, Hall-effect diameter sensing, Lagrange interpolation calibration, ESP32, TMC2209, OLED HMI, MATLAB live monitor.

Introduction

The quality of FDM-printed components is fundamentally constrained by the consistency of the filament used — a dependency that becomes critical in research environments where material properties must be precisely controlled. Despite this, many laboratories rely either on commercially available filaments or incomplete in-house extrusion systems, limiting control over material composition, production parameters, and overall repeatability.

The system available at the start of this work consisted of a partially functional filament extruder capable of melting plastic pellets and producing filament but lacking the necessary infrastructure for reliable operation. The supporting enclosure was mechanically unstable and deteriorating, the wiring was poorly routed and difficult to modify, and no mechanism existed for controlled spooling or feedback. As a result, produced filaments accumulated uncontrollably, leading to tangling, inconsistent handling, and reduced usability.

To address these limitations, a complete system redesign and integration effort was undertaken. A custom modular enclosure was designed and fabricated to provide mechanical stability while allowing easy modification through interchangeable panels, enabling rapid adaptation for additional wiring, sensors, or future system upgrades. The internal wiring was restructured to improve accessibility and maintainability, replacing the previous fixed and constrained layout with a more flexible design.

To enable automated filament handling, multiple sensing methods—including LDR, ultrasonic, and infrared sensors—were evaluated to detect filament position during extrusion. A linear array of light-dependent resistors (LDRs), paired with a controlled laser light source to minimize ambient interference, was selected as the most reliable solution. This sensing system was integrated with a microcontroller-based control unit to dynamically regulate a motorized winding mechanism, ensuring synchronized filament collection. The mechanical winding system was adapted from an existing open-source design (Pasta-lite), with custom motor mounts and couplings developed to interface a stepper motor with the winding mechanism.

All electronics were initially prototyped using a breadboard and later consolidated into a protoboard-based system using an ESP32 microcontroller. The system is powered through a 24 V input with a buck converter stepping down to 5 V for sensors and control logic and utilizes pin-header connections to maintain a modular, plug-and-play architecture.

This report documents the progression from initial system assessment through mechanical redesign, sensor integration, and control system implementation. At the current stage, a functional closed-loop filament extrusion and winding system has been achieved, with ongoing work focused on refining control accuracy and expanding sensing capabilities.

System Overview

The developed system is a semi-automated filament extrusion platform designed to produce and spool filament in a controlled and repeatable manner. It integrates mechanical, sensing, and control subsystems to transform raw plastic pellets into properly wound filament with minimal user intervention. The system operates by continuously extruding molten filament, monitoring its position in real time, and dynamically controlling a winding mechanism to ensure consistent collection.

The overall system is composed of five primary subsystems: the filament extruder, modular enclosure, sensor system, winding mechanism, and control electronics.

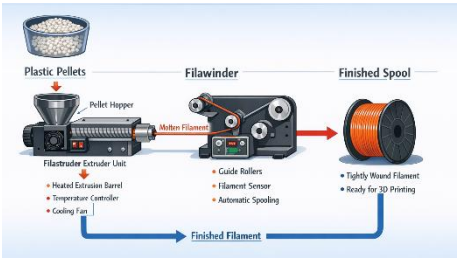

Fig. 1. Pellet-to-filament extrusion and spooling workflow

The extruder is responsible for heating and forming filament from plastic pellets. Surrounding this, a custom-designed modular enclosure provides structural stability while allowing easy access and adaptability for future modifications, including the integration of additional sensors or wiring configurations.

Filament detection is achieved through a sensor system consisting of a linear array of light-dependent resistors (LDRs) paired with a controlled light source, enabling reliable detection of filament position while minimizing the effects of ambient lighting. This information is processed by a microcontroller-based control system, which determines when corrective action is required.

The winding mechanism, adapted from an existing mechanical design, is responsible for collecting the extruded filament onto a spool. It is driven by a motor controlled in response to sensor feedback, allowing synchronization between extrusion and spooling. All subsystems are coordinated through the control electronics, which manage sensor input, execute control logic, and regulate power distribution across the system.

Mechanical System Design

Extruder & Enclosure Design

The mechanical redesign of the filament extrusion system focused on addressing critical limitations in structural integrity, modularity, accessibility, and overall system functionality. The original configuration lacked the rigidity required for stable operation and was only marginally functional in a horizontal orientation. However, for improved filament flow, better integration with downstream components, and more consistent production, a vertical orientation was selected. Prior research has demonstrated that gravitational effects play a significant role in material extrusion processes, where alignment with gravitational forces can improve material flow stability and reduce deformation during extrusion [1]. This supports the use of a vertical configuration in this system, where gravity assists in maintaining a straight extrusion path, minimizing bending and improving downstream handling. This shift significantly increased the importance of structural stability, as the existing casing was unable to maintain alignment or support the extruder under sustained operation. To resolve this, a new enclosure was designed to provide a rigid and stable framework capable of supporting the extruder and associated subsystems without deformation or misalignment.

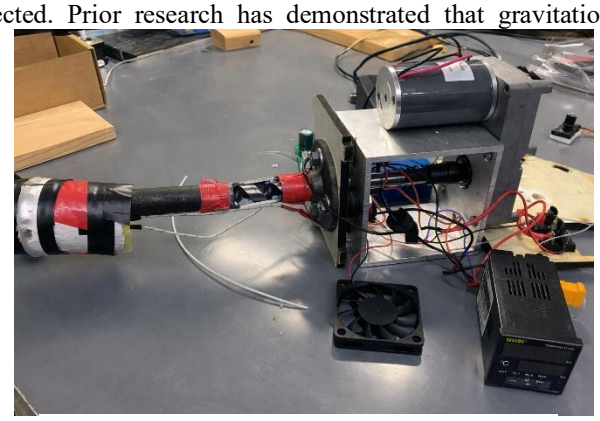

Fig. 2. Original extruder configuration and enclosure limitations (opened)

A key objective of the redesign was modularity. The enclosure was constructed using interchangeable panels that slide into place, allowing individual sections of the system to be removed, modified, or replaced without affecting the entire structure. This approach enables rapid iteration and supports future expansion, such as the integration of additional sensors, improved wiring configurations, or mechanical upgrades. The modular panel system also simplifies customization, as panels can be reprinted with specific features such as mounting points, ventilation openings, or wire-routing channels tailored to evolving system requirements.

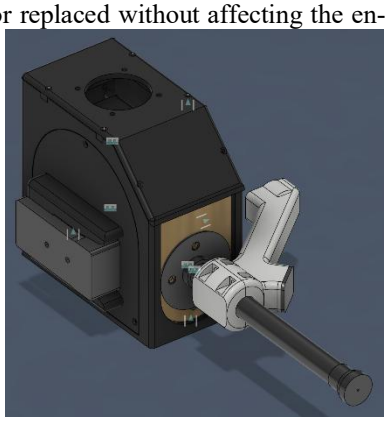

Fig. 3. CAD model of redesigned modular enclosure

Accessibility and maintainability were also significantly improved. In the original system, wiring was routed through tight gaps and permanently soldered in place, making repairs or modifications difficult and often requiring destructive disassembly. In contrast, the redesigned enclosure allows panels to be easily removed, providing direct access to internal components. This enables efficient troubleshooting of electrical or mechanical issues and reduces downtime during maintenance. Internal layout considerations were also improved by organizing wiring paths and securing components in a way that minimizes interference and mechanical strain.

Fig. 4. Removable panel system demonstrating internal

In addition to the enclosure redesign, a custom pellet-feed funnel was developed and integrated directly onto the extrusion pipe. This component serves as the primary interface for material input and was designed with both functionality and modularity in mind. The funnel guides plastic pellets into the extruder while incorporating a threaded connection that allows standard plastic bottles to be attached as material reservoirs. This eliminates the need for a dedicated hopper and provides a simple, scalable solution for increasing pellet capacity. Furthermore, the funnel includes a removable drain mechanism, allowing pellets to be easily emptied when switching materials or performing maintenance, improving overall system usability.

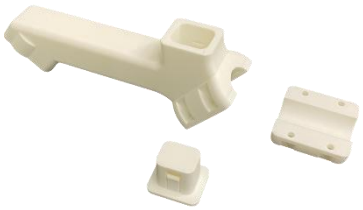

Fig. 5. Custom pellet-feed funnel design

Thermal considerations were also evaluated to ensure the long-term reliability of the redesigned structure. Because the enclosure and several components were fabricated using 3D-printed ABS, it was necessary to verify that heat generated by the extruder would not compromise the structural integrity of the system. Heat transfer testing was conducted along the length of the extruder barrel, from the heated tip to the base where it connects to the enclosure. The temperature was taken using MAX6675 modules connected to thermocouples. These tests confirmed that, despite high temperatures at the extrusion point, heat dissipation along the barrel was sufficient to keep the base plate within safe operating limits. A maximum temperature of approximately 36.5°C was recorded at the mounting interface over extended operation, well below the approximate 90°C threshold for ABS, validating the material choice for the enclosure and mounting components.

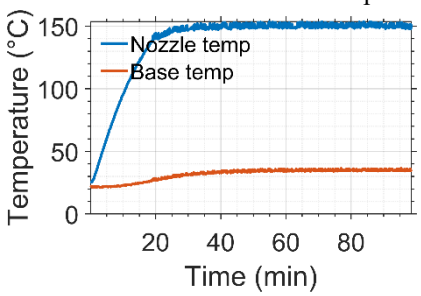

Fig. 6. Temperature distribution along the extruder barrel

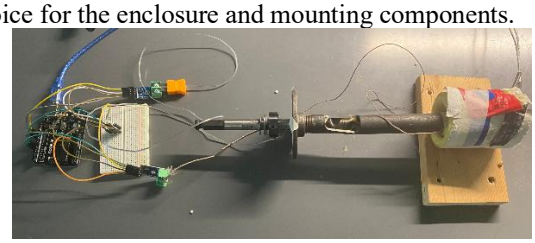

Fig. 7. Experimental setup for thermal measurement using MAX6675 modules and thermocouple sensors

Finally, the mechanical system was designed to support integration with the filament winding subsystem. Mounting features and alignment considerations were incorporated into the enclosure to ensure that the extruded filament could transition smoothly from the nozzle to the winding mechanism without excessive bending or misalignment. These mechanical improvements collectively provide a stable, adaptable, and maintainable platform that supports reliable filament production and serves as a foundation for further system enhancements.

Filament Winding Mechanism

A filament winding mechanism was required to address the limitations of the original system, where extruded filament accumulated on the ground, leading to tangling and inconsistent handling. To resolve this, a winding system based on the "Pasta-lite" filament winder was implemented. This design utilizes a lead screw-based traverse mechanism to guide the filament back and forth across the spool, ensuring even distribution and reducing the risk of overlap or misalignment.

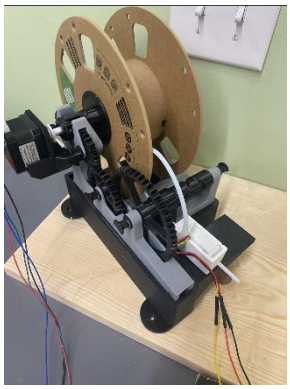

Fig. 8. Pasta-lite model

To integrate this mechanism, a custom mount was designed to attach a NEMA 17 stepper motor, along with a coupling interface to connect the motor shaft to the hexagonal input of the winding system. The stepper motor enables controlled rotation, allowing the winding speed to be adjusted in response to filament conditions.

This integration provides a reliable and repeatable method for filament collection, improving overall system performance and supporting closed-loop control of the extrusion and winding process.

Sensor System & Evaluation

Sensor Requirements

A critical component of the filament extrusion system is the ability to reliably detect filament presence and slack during operation. This sensing capability enables closed-loop control of the winding mechanism, preventing issues such as filament tangling, slack accumulation, or inconsistent spooling. Given the small diameter of the filament (approximately 1.75 mm), the sensing system was required to detect a thin and fast-moving target with high precision.

To meet system requirements, the selected sensor needed to provide fast response times to react to sudden changes in filament position, as well as consistent performance under varying environmental conditions. In particular, the sensor had to operate reliably despite changes in ambient lighting and filament material properties. Additionally, the sensing method needed to support real-time feedback suitable for integration into a control system, while remaining cost-effective and easily replaceable for long-term maintainability.

Sensor Testing & Comparison

To determine the most suitable sensing approach, multiple sensor types were evaluated through experimental testing. These included a laser-based speed module, an ultrasonic distance sensor, and an infrared (IR) obstacle detection sensor.

Each sensor was tested using a microcontroller-based setup, and performance was assessed based on response time, reliability, sensitivity to filament size, and susceptibility to environmental noise.

The laser speed module demonstrated fast response and was largely insensitive to material properties; however, it lacked the ability to provide meaningful distance or positional feedback, limiting its usefulness for closed-loop control. The ultrasonic sensor could measure distance, making it theoretically suitable for detecting filament slack. However, due to the small diameter of the filament, the sensor exhibited inconsistent readings and slower response times, reducing its reliability for real-time control. The IR obstacle sensor provided fast detection but was highly sensitive to ambient light conditions and filament color, resulting in frequent false triggers and unstable operation.

A summary of these results is shown in Fig. 9, with a comparison of sensor performance highlighting the trade-offs between detection accuracy, speed, and environmental robustness. Overall, none of the tested standalone sensors provided the combination of precision, reliability, and responsiveness required for this application.

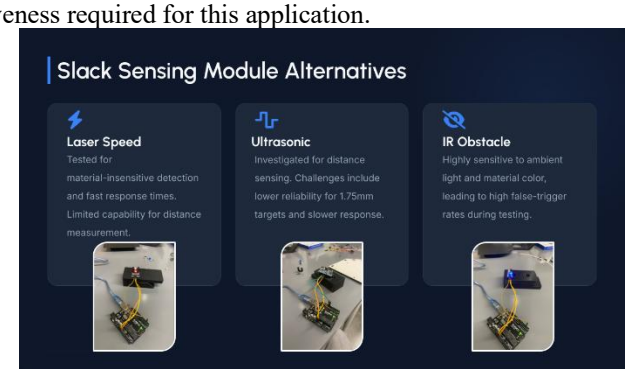

Fig. 9. Test setups and comparison of evaluated sensor modules

Final LDR-Based Detection System

Based on the limitations observed in the initial testing phase, an optical sensing approach using light-dependent resistors (LDRs) paired with a laser line source was selected as the final solution. This method provides precise detection of filament position by monitoring changes in light intensity as the filament passes through a controlled optical path.

The implemented system consists of a linear array of five LDR sensors aligned with a 1W red line laser. The laser provides a consistent and focused light source, allowing the sensors to respond specifically to the known light intensity rather than ambient lighting conditions. When filament passes between the laser and the sensors, it partially blocks the light, causing a measurable change in resistance. By monitoring these changes across multiple sensors, the system can determine filament position and detect slack conditions in real time.

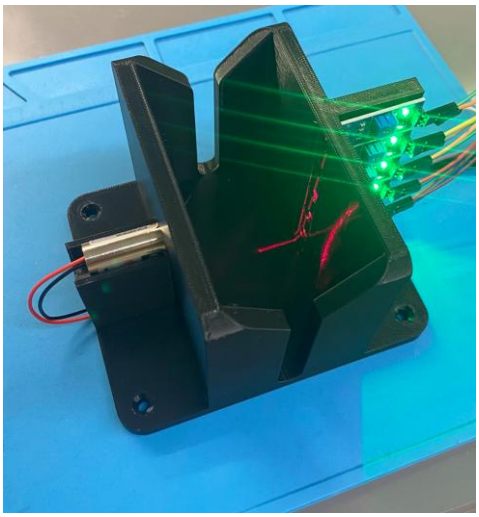

Fig. 10. Final LDR sensor module

This multi-sensor configuration improves reliability compared to a single sensor by providing spatial resolution and redundancy, reducing the likelihood of false detections. Additionally, the use of a controlled laser source minimizes interference from environmental lighting, addressing one of the primary weaknesses observed in the IR-based approach.

The sensor array is mounted within a custom-designed holder that ensures consistent alignment between the laser and LDRs while maintaining proper spacing for accurate detection. This mechanical integration is critical to ensuring repeatable performance and long-term stability of the sensing system. The sensor output is processed using threshold-based logic within the microcontroller, enabling real-time detection of filament position changes and triggering the winding motor when slack conditions are detected.

Control System & Electronics

System Architecture

The control system is designed to enable closed-loop regulation of the filament winding process by continuously monitoring filament position and adjusting motor behavior accordingly. The overall architecture consists of three primary components: the sensor array, the microcontroller unit, and the motor actuation system.

The LDR-based sensor array provides real-time input on filament position, which is processed by an ESP32 microcontroller. Based on this input, the microcontroller determines the appropriate response and generates control signals for a stepper motor driver. The motor then adjusts the winding speed to maintain proper filament tension and prevent slack accumulation. This feedback loop enables autonomous operation with minimal user intervention.

Microcontroller Implementation

The control logic is implemented on an ESP32 microcontroller, selected for its processing capability, flexibility, and prior integration experience. The microcontroller reads

digital inputs from a five-sensor LDR array, where each sensor corresponds to a discrete filament position level.

Sensor inputs are mapped to five vertical levels, ranging from excessive slack (lowest level) to over-tight conditions (highest level). Each sensor outputs a digital signal, where a HIGH state indicates that the filament is blocking the laser path. The ESP32 continuously scans these inputs to determine the current filament position and updates system behavior accordingly.

The motor is controlled using a NEMA 17 stepper motor driven by a TMC2209 driver module. For simplicity and reliability, the driver is operated in step/direction mode rather than UART configuration. The ESP32 generates step pulses and direction signals directly, allowing precise control over motor speed without requiring advanced driver configuration.

Control Logic

The system operates using a discrete, level-based control strategy combined with a state machine to ensure safe and predictable behavior. The five sensor levels define the operating conditions of the system:

- Level 5: Over-tight filament → fault condition (system stops)
- Level 4: Filament is near optimal tension → motor stops
- Level 3: Slight slack → motor runs at slow speed
- Level 2: Increased slack → motor runs at high speed
- Level 1: Excessive slack → fault condition (system stops)

To improve reliability, a debounce mechanism is implemented to ensure that sensor reading remains stable for a minimum duration before being accepted. This prevents false triggering due to noise or transient disturbances.

Motor control is implemented using non-blocking logic, allowing simultaneous sensor monitoring and motor actuation. A ramping function is used to gradually adjust motor speed by modifying the step interval, preventing sudden changes in motion that could introduce mechanical stress or instability. When transitioning from a stopped state, the motor begins at a low speed and ramps toward the target speed, ensuring smooth operation.

Additionally, a startup validation routine ensures that filament is present within a valid operating range before enabling the motor driver. If the system detects invalid conditions—such as no filament or extreme slack—it enters a fault state, disables the motor, and requires a manual reset. This behavior enhances safety and prevents damage to the system.

Power System

The system is powered by a single 24 V input supply, which provides energy for both the motor and control electronics. A buck converter is used to step down the voltage to 5 V for the ESP32 and sensor modules. This approach simplifies the power architecture while ensuring that all components receive appropriate operating voltages.

Separating the high-power motor supply from the low-voltage control electronics through regulated conversion helps improve system stability and reduces the risk of voltage fluctuations affecting sensor reading or microcontroller operation.

Prototyping and Integration

The control system was initially developed and validated using a breadboard-based prototype, allowing rapid testing of sensor configurations and control logic. During this phase, jumper wires and temporary connections were used to facilitate quick iteration and debugging.

Following successful validation, the system was transitioned to a protoboard implementation to improve reliability and durability. Pin headers were incorporated to allow modular connections between components, enabling plug-and-play functionality for sensors, motor drivers, and power connections. This design choice aligns with the overall system goal of modularity and maintainability, allowing components to be easily replaced or upgraded without extensive rework.

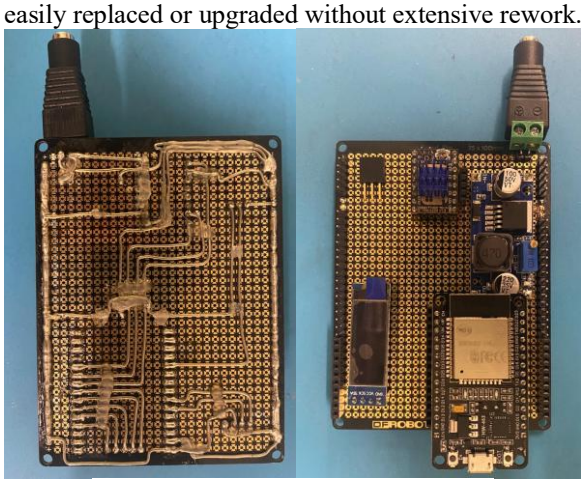

Fig. 11. Protoboard wiring and modules

System Integration & Validation

All major subsystems — the mechanical structure, the filament winding mechanism, the five-LDR slack array, and the control electronics — were assembled, individually verified, and integrated into a single platform. The transition from the breadboard prototype to a permanent protoboard exposed several short circuits between adjacent solder pads, which were identified by multimeter probing and resolved by reflowing the affected joints and isolating the densest cross-rail regions in non-conductive hot glue. Post-fix verification confirmed that the 24 V supply reaches only the TMC2209 power input and the buck converter, that the ESP32 and all logic peripherals see no more than 5 V, and that no leakage path exists between rails.

After the electrical fix, the full system was assembled inside the modular enclosure and operated as a single unit. The pellet-load → extrusion → slack feedback → winding chain ran autonomously without operator intervention at the controller level, the OLED reported the expected state transitions, and the diameter sensor streamed calibrated samples to the MATLAB live monitor. The system reached the integration milestone described qualitatively in the mid-term as in-progress and was then advanced into the quantitative validation phase documented in Section VII.

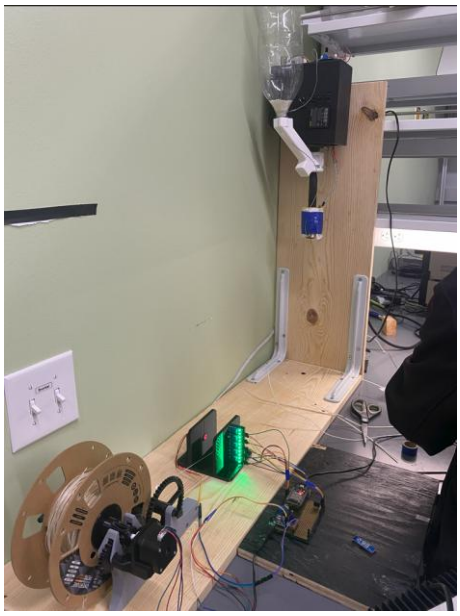

Fig. 12. Assembly of full extrusion system

Extrusion-Rod Restoration

The two inherited extrusion rods were both seized by hardened plastic from prior runs. One rod was visibly bent and was retained as a backup. For the working rod, a heat gun was applied in 30-minute intervals to bring the barrel above the PLA softening point, after which the screw could be separated from the barrel. The screw was scraped clean, the residual film inside the barrel was extracted, the nozzle was removed for tip cleaning, and the unit was reassembled inside the enclosure.

The first post-restoration run produced filament at approximately 2.8 mm — the rod had shipped with the wrong nozzle. The 1.75 mm nozzle was recovered from the second (bent) barrel, transferred onto the working rod, and verified to produce filament near the 1.75 mm target on the next run. This restoration recovered both inherited rods to a usable state and unblocked the parameter sweep documented in Section VII.

Auxiliary Mechanical Additions

Three printed aids were introduced after the system began running end-to-end:

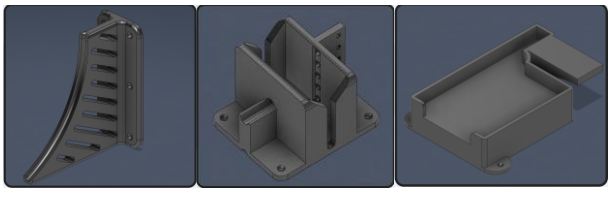

Fig. 13. From Left to Right: Filament Guide Rail, LDR Module, FilaWinder Booster

Filament guide rail: a sloped guide that contains the filament between the nozzle and the slack tower and gradually curves it into the sensor path, reducing the effect of gravity-driven sway and the diameter-measurement artifacts it produces.

LDR module, version 2: a funnel-style entry geometry was added to the LDR housing after the original module allowed the filament to wander close enough to the laser to shadow multiple sensors simultaneously. Version 2 forces the filament onto the central axis.

FilaWinder booster: a 3D-printed riser that fixes the winder at the optimal height relative to the enclosure exit and improves take-up tension consistency.

Diameter Sensing — AH3503 Hall-Effect Probe

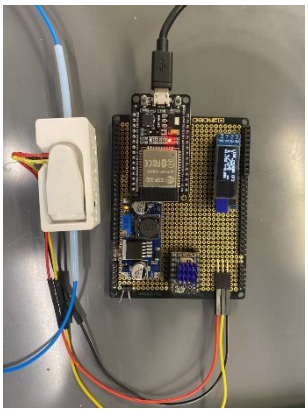

Fig. 14. Diameter Sensor

To measure live filament diameter the system uses an AH3503 linear Hall-effect sensor mounted in a printed fixture through which the freshly extruded filament passes. The sensor reads the ferromagnetic perturbation produced by a nearby permanent magnet against the filament cross-section and is sampled by ADC1 on GPIO 35. Because the analog response is non-linear with diameter, a three-point quadratic calibration is performed against targets defined in firmware as 0.00, 1.40, and 1.75 mm. The three corresponding raw readings are converted into quadratic coefficients (A, B, C) by Lagrange interpolation, after which subsequent samples are reduced to diameter by $d = A \cdot r^2 + B \cdot r + C$. Coefficients and raw calibration values are persisted in NVS through the ESP32 Preferences library and survive a power cycle.

A 30-sample (≈ 3 s at the 10 Hz emit rate) rolling window provides on-device statistics — mean, min, max, and half-spread — which feed both the OLED Stats screen and the ± precision badge displayed in Production mode.

Integrated Firmware v1.0

The mid-term firmware was a blocking single-purpose slack sensor. The final firmware (Filament_System.ino, ≈ 1100 lines) consolidates every peripheral into a single application structured around a seven-state state machine: ST_MENU (top-level menu, shown at startup and after any recoverable fault), ST_PRODUCTION (closed-loop run: slack ladder drives the winder; diameter is displayed and optionally streamed), ST_LIVE_READ (diameter telemetry only; the winder is held off so a length of filament can be characterized in isolation), ST_CAL_FLOW (three-point quadratic calibration walked through one target at a time), ST_INFO and ST_STATS (pin-map, firmware version, and rolling-window statistics for the current session),

ST_SPEED_CFG (operator override of the slow and fast step intervals — default 10 000 µs ≈ 100 sps and 2 500 µs ≈ 400 sps — persisted to NVS), and ST_RESET_CONFIRM (guarded entry to factory-reset NVS storage).

Fig. 15. Firmware Modes

Per-frame work is non-blocking. The slack-level reader applies a 50 ms debounce window; level changes are dispatched only after the same level has been observed continuously for the debounce interval, which suppresses the chatter that the original blocking waitForFilament() prototype produced when the filament transited a sensor boundary. Step-rate transitions go through a soft ramp so the winder never jumps directly from zero to fast, which previously caused the TMC2209 to mis-step under load. Faults disable the driver (EN_PIN high), park the state machine in ST_MENU, and require explicit operator acknowledgement before re-enabling the winder — replacing the hard-reset behavior of the earlier prototype. The current firmware requires a direct connection to the ESP32 and communication through a compatible IDE. Future revisions will include dedicated hardware controls and an onboard menu interface.

The diameter pipeline samples the AH3503, applies the calibrated quadratic, pushes the result through a 30-sample rolling window, and emits a single ASCII line every 100 ms (10 Hz) to USB serial. The OLED draws are I²C-probed at boot — if the display is absent the firmware silently falls back to serial-only operation rather than blocking on a non-acknowledging I²C transaction.

Extrusion Validation Results

Method

Once the system was running end-to-end, extrusion temperature and winder speed were swept across the PLA processing window. Three set-point temperatures (190, 200, 210 °C) were each combined with four winder speeds (25, 50, 75, 100 % of DEFAULT_FAST = 400 sps). For each combination the steady-state diameter was sampled across three short (≈ 30 s) segments and inspected against a 1.75 mm reference. Combinations whose diameter measurement was qualitatively unstable — i.e., never settled within an interpretable band — were marked x and excluded from numerical analysis.

Parameter-Sweep Results

Speed \ Temp	190 °C	200 °C	210 °C
25 %	x	x	x
50 %	x	x	1.67, 1.72, 1.82
75 %	x	1.75, 1.85, 1.99	1.67, 1.72, 1.89
100 %	x	1.77, 1.83, 1.87, 1.91	1.81, 1.84, 1.91

Table I. Filament diameter (mm) by extrusion temperature and winder speed.

The 190 °C row never produced an interpretable measurement; the melt was too cool to flow consistently. 100 % winder speed at 195 °C (interpolated between the 190 °C and 200 °C bracket) was selected for the verified live runs because it produced the tightest cluster among the trial points actually recorded.

Live Spool Runs

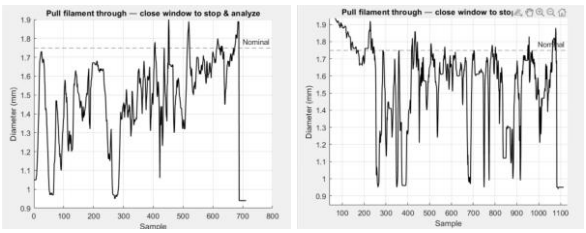

Fig. 16. From Left to Right: 210*C, 195*C

Two ≈ 20-minute runs were executed at 100 % winder speed, one at 210 °C and one at 195 °C, with the AH3503 streaming diameter to MATLAB at 10 Hz through diameterMonitor.m. Each run produced approximately one meter of filament. The MATLAB script reads COM5 at 115 200 baud, draws a live animatedline plot, and on figure-close prints a quality report — sample count, mean, 1σ spread, worst-case deviation from mean, min/max, and offset against the 1.75 mm nominal — and renders a histogram for distribution sanity-checking.

Control Run — Commercial ABS

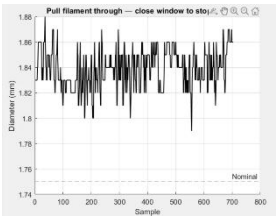

Fig. 17. Manufactured ABS

The same MATLAB pipeline was run against a commercial spool (ABS Overture, nominal 1.75 mm, vendor tolerance ± 0.05 mm) pulled by hand through the diameter probe. The control trace sits ≈ 0.09 mm below the nominal value, which is interpreted as a residual mechanical offset of the diameter sensor relative to the 1.75 mm reference. After subtracting that offset the control distribution is consistent with the vendor tolerance.

Discussion

Two findings dominate the validation results. First, the control run quantifies a 0.09 mm static offset in the diameter

probe. This is small relative to the half-window 0.05 mm tolerance and is fully absorbed by the three-point quadratic calibration when calibration is performed against a known reference at startup, which is now the recommended operating procedure. It is not a sensor-noise problem — the within-spool spread on the control run is roughly ±0.03 mm, consistent with the precision badge displayed by the OLED in Production mode.

Second, even after offset correction the experimental spools show diameter excursions an order of magnitude larger than the control spread. The dominant cause is non-uniform tension at the spooler: with no bearing-supported guide the filament wandered between the nozzle and the sensor tower, perturbing the pull rate, and a perturbed pull rate changes the local cross-section while the polymer is still soft. The diagnosis is consistent with the closed-loop slack ladder doing its job — the winder ramps faster when slack accumulates and slower when the path tightens — but the open-loop variable in the chain is the geometry of the path itself, not the control logic. The natural next step is therefore a bearing-supported guide rail rather than further controller tuning.

Limitations

Diameter ground truth is single-spool. The control distribution is derived from one commercial spool; a more complete calibration would average several known spools.

Temperature setpoint is open-loop. The MAX6675 was used to validate enclosure thermals during the mid-term phase, but the production firmware does not yet close the loop on heater temperature; the FilaStruder retains its native PID controller.

Single-material characterization. Quantitative results in Section VII are PLA only. ABS was used only as a calibration reference, not as an extrusion test.

Drive mode. The TMC2209 is operated in STEP/DIR/EN with MS1/MS2 strapped for 1/8 microstepping; UART configuration is not used and stallGuard is not exposed.

Future Work

Bearing-supported guide rail between nozzle and sensor tower to remove the dominant remaining source of diameter variance.

Closed-loop nozzle temperature by promoting the MAX6675 thermocouple to a firmware-level PID input, allowing the OLED to expose temperature setpoint alongside winder speed.

Composite-filler trials. With the platform repeatable, the lab can begin extrusion of magnetic and conductive composite formulations toward soft-actuator embedded actuation.

Conclusion

The platform has moved from an inherited, partially functional, open-loop bench setup into a closed-loop, vertically oriented, modular extrusion system with live diameter feedback, persistent calibration, an OLED operator interface, and a reproducible MATLAB-side analysis path. The main qualitative claim of the mid-term — that the system would close the loop and become operator-friendly — is now backed by quantitative validation: a parameter sweep that identified 195 °C × 100 % winder speed as the optimum, two live spool runs with streamed diameter data, and a control run that bounds the sensor's intrinsic precision at roughly ±0.03 mm. The remaining diameter variance traces to a mechanical guide-rail upgrade rather than to the controller, and the lab is now positioned to use this platform as the starting point for composite-material research.

Acknowledgements

The author thanks Prof. Yonas Tadesse for his sustained support of the project and access to the RIDE Research Laboratory, and Imranuddin Syed (graduate mentor) for technical guidance and on-site collaboration during sensor selection, protoboard debugging, and parameter-sweep testing.

[1] “High-gravitational effect on process stabilization evaluation for material extrusion using PLA filament,” Scientific Reports, 2025. [Online]. Available: https://www.nature.com/articles/s41598-025-06028-3

[2] “Understanding ABS Heat Resistance: A Comprehensive Guide,” Wevolver. [Online]. Available: https://www.wevolver.com/article/understanding-abs-heat-resistance-a-comprehensive-guide